

Responses of auditory-nerve fibers to multiple-tone complexes

Li Deng and C. Daniel Geisler

Department of Neurophysiology and Department of Electrical and Computer Engineering, University of Wisconsin—Madison, Madison, Wisconsin 53706

Steven Greenberg

Department of Neurophysiology, University of Wisconsin—Madison, Madison, Wisconsin 53706

(Received 16 December 1986; accepted for publication 2 September 1987)

To relate level-dependent properties of auditory-nerve-fiber responses to nasal consonant-vowels to the basic frequency selective and suppressive properties of the fibers, multitone complexes, with the amplitude of a single (probe) component incremented, were used as stimuli. Quantitative relations were obtained between the systematic increase of fiber synchrony to the probe tone and the decrease of synchrony to CF, as the amplitude of the probe tone was increased. When such relations are interpreted as a measure of fiber frequency selectivity based on a relative synchrony criterion, a breadth of frequency tuning is obtained, at a 70-dB SPL multitone sound-pressure level, which is generally broader than that of the fiber's threshold tuning curve. Quantitative comparisons with the same fiber's responses to the nasal speech sounds indicate that the fiber's speech responses share some common features with its probe-tone responses.

PACS numbers: 43.63.Pd, 43.71.Cq

INTRODUCTION

The ability of the inner ear to perform a type of spectral analysis has been known for a long time. There are ample data at the level of auditory-nerve discharges to show that this analysis is very complicated, involving such nonlinearities as "two-tone synchrony suppression," whereby adding a second tone reduces the strength of the discharge synchrony to the original tone (e.g., Arthur, 1976; Javel *et al.*, 1983). Such suppressive effects have also been shown psychoacoustically in a variety of forms, including lateral suppression (Houtgast, 1974) and tones masking noise (Schroeder *et al.*, 1978). All these point to the nonlinear features of the auditory system in carrying out spectral processing of complex sounds.

As described in the first article of this series (Deng and Geisler, 1987a), intensity-dependent nonlinearities have also been observed in the responses of auditory-nerve fibers to speech sounds. In particular, we found that for utterance-initial nasal consonants presented at conversational intensities (about 70 dB SPL) one low-frequency formant tends to dominate the response synchrony of many fibers. In the last article of this series (Deng and Geisler, 1987b), we show that this domination, in many cases, cannot be accounted for by the frequency sensitivity exhibited by the fibers' threshold tuning characteristics.

The present article attempts to explore this type of nonlinearity more systematically, by using a particular type of multitone sound complex in which the amplitude of a single component is incremented. These stimuli, having been used in the "profile analysis" of psychophysics (Green, 1983), serve as a powerful means of quantitatively exploring the effects of spectral contrast in determining the firing patterns of auditory-nerve fibers, and provide further insight into the nature of peripheral auditory nonlinearities. The complexity

of these stimuli lies somewhere between that of speech and of two-tone signals, for which an abundance of experimental data is already available. It will be shown that the nature of the suppression observed in the responses of the auditory-nerve fibers to such sounds can account in large measure for the formant-dominant responses we reported in the first article.

I. METHODS

The surgical preparation, sound delivery and calibration system, and the neural recording procedures were identical to those described in the preceding article (Deng and Geisler, 1987a). The results included in this chapter are from two healthy adult cats, C85134 (experiment "A") and C85088 (experiment "B"), from which much of the data reported in the first article were also obtained.

A. Generation and presentation of multitone stimuli

The main stimulus used in this study comprised 60 sinusoidal tones (which we designate a *multitone complex*) whose frequencies were 60 successive integer multiples of 122.07 Hz. This fundamental frequency (F_0) is within the range of typical male voiced speech pitch (Pickett, 1982) and was chosen to minimize windowing errors in our fast Fourier transform (FFT) analyses.¹ The amplitude of one of the tones, called a "probe" component, was incremented by variable amounts. The amplitudes of the remaining 59 tones were all kept equal and constant. The amplitude and frequency (F_p) of the probe component were controlled by the experimenter. In one condition, when the amplitude of the probe tone was set equal to that of the other tones, sounds with a "flat" spectral envelope were generated, which can be used to estimate the frequency selectivity of the auditory-nerve fibers (Smooenburg and Linschoten, 1977; Evans,

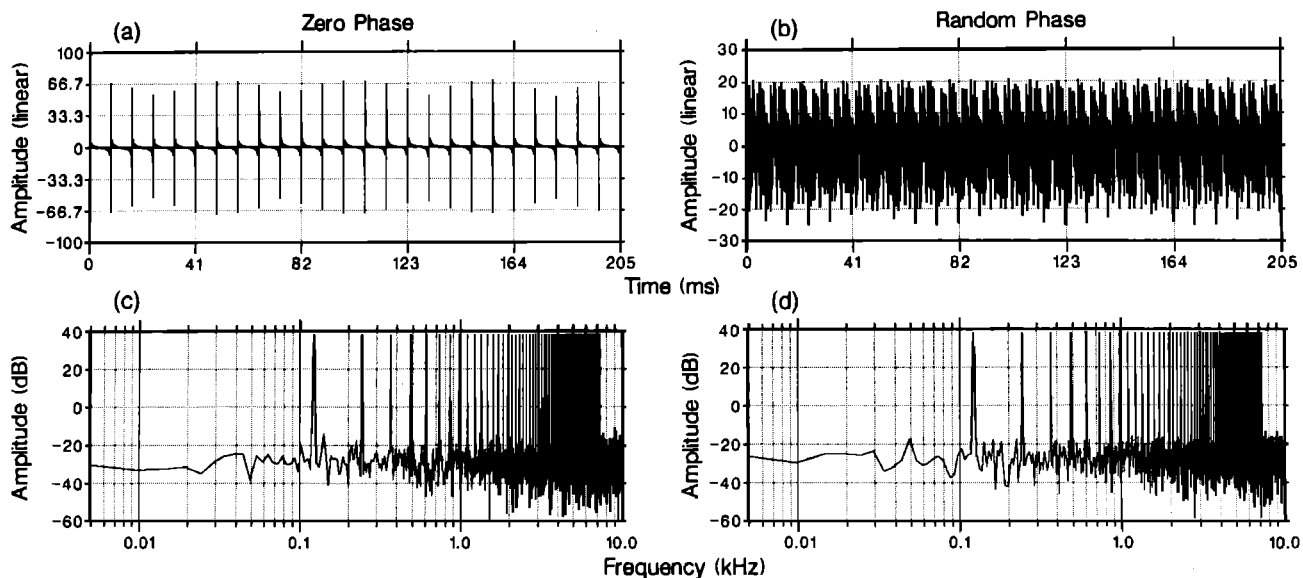


FIG. 1. Waveforms and spectra of 60-component multitone complexes. (a) Waveform of zero-phase complex. (b) Waveform of random-phase complex. (c) Amplitude spectrum of zero-phase complex. (d) Amplitude spectrum of random-phase complex. The fundamental frequency (F_0) is 122.07 Hz.

1985). The waveforms and FFT spectra of such flat-spectrum signals are shown in Fig. 1 for two different phase relationships: all zero sine phases [Fig. 1(a)] and random phases [Fig. 1(b)]. Note that both sounds have identical amplitude spectra and an identical fundamental period of 8.192 ms [Fig. 1(c) and (d)].

The calibration data of the acoustic system were used to insure that each component in the flat-spectrum signal had the same SPL. An equivalent SPL for the entire flat-spectrum composite signal was calculated by adding the acoustic energies of all 60 components and then determining the amplitude of a single sinusoidal waveform that possessed that same total energy. This equivalent intensity was generally around 70 dB SPL (at which intensity each component has a peak value of 52.2 dB SPL). The amount that the probe tone's amplitude was incremented above the others in the flat-spectrum signal will be expressed in terms of decibels. For reasons of speed and flexibility, the addition of the probe tone's amplitude increment was done computationally online during the experiment. All of the stimuli were synthesized in a Harris/5 computer and delivered through a digital stimulus system (Rhode, 1976) to a Stax earphone.

B. Data analysis

Because all of the multitone stimuli were periodic with a period of 8.192 ms, the resulting neural discharge patterns were quasiperiodic, despite such temporal effects as adaptation. This allowed us to analyze fiber responses in terms of period histograms (PHs) (Rose *et al.*, 1967), which provide estimates of response synchrony that have less variance than those obtainable directly from post-stimulus-time (PST) histograms (for more detail, see Deng, 1984). Only standard PHs, not "compound PHs" (Goblick and Pfeiffer, 1969), were used.

The FFTs of the PHs were calculated to determine the synchronization strength of the fiber's firing pattern to each frequency component. Alternatively, the "vector strength"

(Goldberg and Brown, 1969), which is equivalent to the ratio of the FFT spectral amplitude at the desired harmonic over the dc value, was also calculated. Because the intensity of our multitone stimulus (about 70 dB SPL) was near or above the discharge-rate saturation level for most fibers, even a large increment of the amplitude of the F_p component did not change the discharge rate significantly (except for occasional cases of rate suppression). Hence, the synchrony measures using vector strength do not reflect "spurious synchrony suppression" attributable to waveform rectification (Greenwood, 1986).

II. RESULTS

A. Response synchrony evoked by phase-coherent multitone signals (zero-phase angles)

As an example of our results, a comprehensive set of response PHs to zero-phase multitones, with the amplitudes of different probe-tone components incremented by various amounts, is shown in Fig. 2. All of these data were collected from a single fiber, A16. Its CF, determined from its threshold frequency tuning curve, was approximately 2600 Hz, closest to F_0 's 21st harmonic, 2563.5 Hz. At CF, the fiber's rate threshold was 13 dB SPL. The intensity level of the flat-spectrum sound was 70 dB SPL. Each column contains PHs gathered in response to the multitone stimulus with one particular component serving as the probe tone. That component's amplitude was incremented in 2- or 3-dB steps, as indicated in the figure. For notational convenience, in all the following figures, 0 dB has been assigned to the level of each component in the flat-spectrum signal. The value of F_p , always at some harmonic of F_0 (122.07 Hz), is indicated at the top of each column.

Several properties of these PHs are striking. First, in response to stimuli with small probe-tone amplitude increments (e.g., the bottom row), discharges tend to cluster

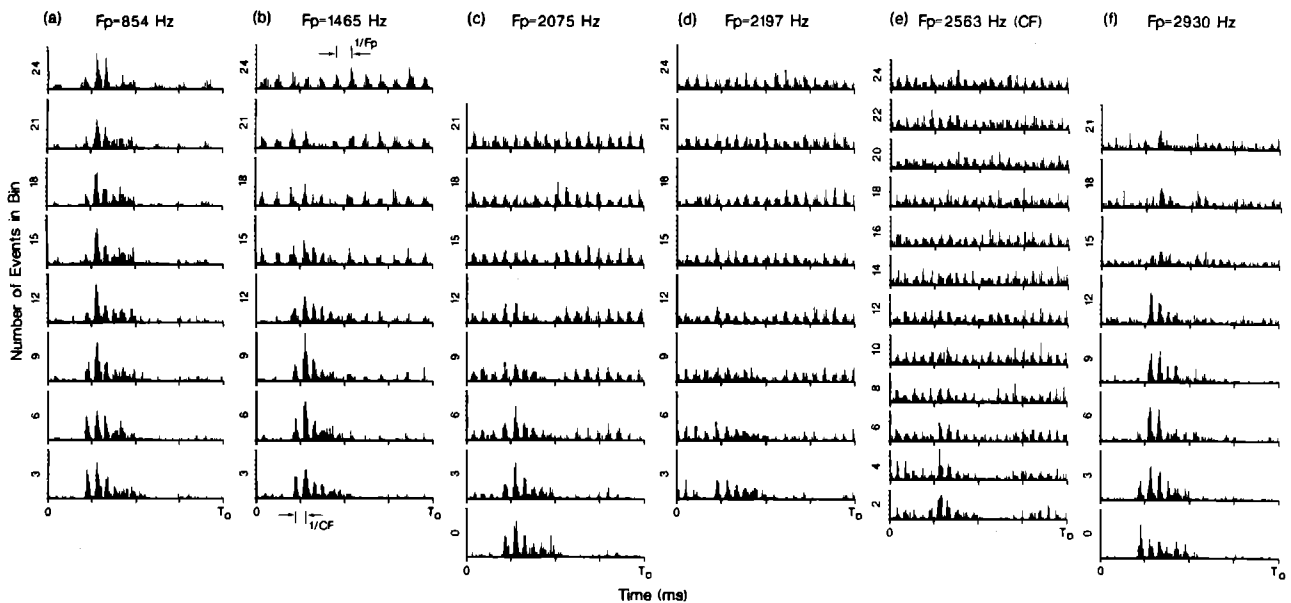


FIG. 2. A series of period histograms (PHs), for fiber A16, in response to zero-phase multitone complexes for six different probe frequencies (F_p 's). Each column contains data for one F_p , indicated at the top of that column. The amount of increment (in dB) of the amplitude at F_p , relative to a flat spectrum, is indicated on the ordinate of each PH. The CF of A16 (2600 Hz) is near the 21st harmonic of F_0 (2563.5 Hz). The abscissa of each PH extends over one period (T_0) of the fundamental (F_0). Spontaneous rate varied from 25.2–32.4/s.

within a small portion of the fundamental period, indicating a high degree of synchrony to F_0 . This response pattern is a consequence of the highly peaked nature of the zero-phase multitone stimulus, similar to a train of double-sided pulses [cf. Fig. 1(a)]. The fiber tends to respond vigorously to these pulses, acting like a lightly damped bandpass filter. The fiber, in fact, had moderately sharp tuning (Q_{10} of 4.5). Second, certain regular intervals between adjacent discharge peaks are apparent in all PHs. At low probe-amplitude increments, the intervals are approximately $1/CF$ in duration. At high probe-amplitude increments, however, these intervals are approximately equal to $1/F_p$. Further, the transition point between the $1/CF$ intervals and the $1/F_p$ intervals is highly dependent on F_p . As F_p moves away from CF, this transition occurs at increasingly higher probe-tone intensities. For instance, in column (a), where F_p is 854.5 Hz, far below the CF, even a 21-dB increment does not change the timing pattern of the PH significantly.

Third, as the level of the amplitude increment increases, the discharges tend to spread over the entire fundamental period, indicating a reduction in the strength of synchrony to F_0 . The dependency of such a transition upon F_p also follows a consistent trend: It occurs at lower increments if F_p is close to CF, and at higher increments if distant from CF. Finally, probe tones with F_p 's higher than CF are less effective in dominating the timing pattern than those with F_p 's below CF. This can be seen by comparing waveforms in columns (d) and (f). In both instances, the F_p differs from CF by 366.21 Hz. Changes in the general shape of the PHs, their periodicities, and the reduction of their discharge clustering all occur at much lower increments in column (d) than in column (f).

The above observations can also be demonstrated by measuring the spectral amplitudes of each PH with FFT analysis, as shown in Fig. 3. The disappearance of clustering

within a portion of the fundamental cycle that was seen in Fig. 2 corresponds, in this figure, to a reduction in the amplitude of F_0 (the lowest nonzero frequency shown in each spectrum). Likewise, changes of the major interval or the periodicity observed in the PHs of Fig. 2 correspond to movements of the peak amplitudes in the FFTs of Fig. 3.

At the bottom of each column in Fig. 3, the vector strengths of three different frequency components are shown as functions of the increment of the probe-tone amplitude. The F_p component is indicated by asterisks, the harmonic component nearest to CF is indicated by triangles, and the fundamental component F_0 is indicated by square symbols. The trends described above are now quantitatively measurable. For example, the amplitude of the F_p response component becomes equal to that of the F_0 response component at an extrapolated intensity increment of 4.8 dB when F_p is 2075 Hz [Fig. 3(c)], but a 27.4-dB increment is needed to achieve the same equality when F_p is 854 Hz [Fig. 3(a)].

Reasonably large sets of responses were obtained from six other fibers using zero-phase multitone complexes. These data (Deng, 1986) came from fibers having a wide range of CFs (0.2–3.5 kHz), all with normal rate thresholds at CF (Lieberman, 1978). In general, the response characteristics follow quite well the trends just described.

B. Response synchrony produced by random-phase multitone complexes

A series of PHs and their FFTs showing fiber A16's responses to a *random-phase* multitone complex with an F_p of 2075 Hz is shown in Fig. 4. In many respects, the PHs in column (a) of the figure are very similar to those in the corresponding column (c) of Fig. 2, both of which involved the same F_p . Periodicities corresponding to $1/CF$ are seen in the lower plots of both columns, while $1/F_p$ intervals dominate the upper plots. However, there is one major difference

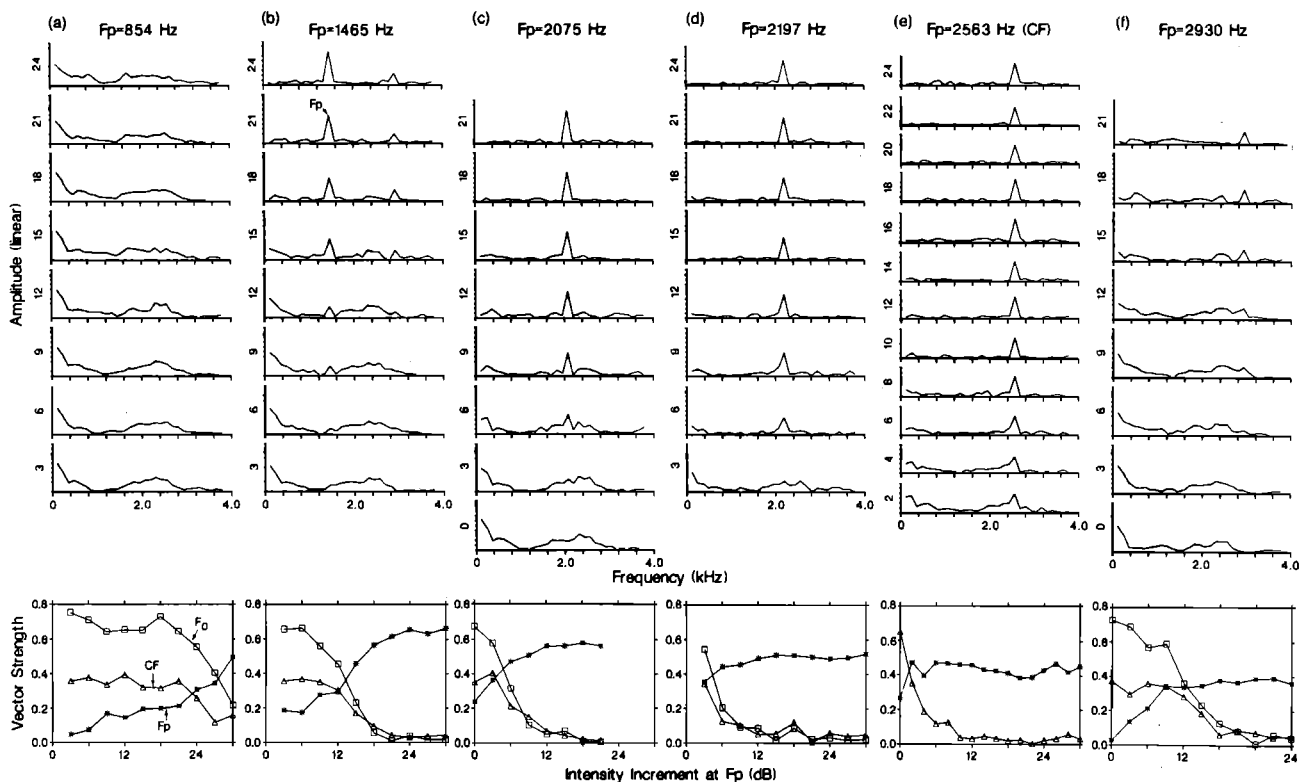


FIG. 3. Magnitude spectra of the PHs in Fig. 2, in the same format as Fig. 2. The summary plot at the bottom of each column shows the relationships between the vector strengths of three frequency components and the amplitude increment at F_p . These frequency components are F_p , F_0 , and the harmonic whose frequency is nearest to CF (labeled CF in brief), indicated by asterisk, square, and triangle symbols, respectively. Note that a decline of synchrony to F_0 and CF occurs simultaneously with the increase of the synchrony to F_p as the amplitude increment at F_p increases.

in the responses to the two signals. Marked differences in the degree of peakedness characterize the waveforms in the lower plots of the respective columns, with the zero-phase condition producing much more peaked PHs. This is a consequence of the much more peaked nature of the zero-phase stimuli (cf. Fig. 1). The result is a much lower value of the F_0 frequency component at the smaller increments of the random-phase condition [cf. Fig. 3(c)].

We recorded significant amounts of data using random-phase multitone complexes from three other fibers. The trends observed in fiber A16's responses are representative of the responses of the other fibers.

C. The "Isocapture" curve as an estimate of a fiber's frequency selectivity

Information concerning the effectiveness of a multitone stimulus' spectral peak in dominating ("capturing") the periodicities of the response discharges is presented in Fig. 3. This capturing effect is functionally significant in that it allows the discharge patterns of a fiber that is not itself tuned to the frequency of the stimulus' spectral peak to be dedicated to encoding that spectral component. Moreover, certain fundamental properties of the peripheral auditory system emerge from such capture data. As seen in Fig. 3, a decline in synchrony to CF always accompanies a simultaneous increase of synchrony to the probe frequency F_p . The crossover point between these two curves is where the probe component just starts to dominate the response synchrony. In the above example, the probe-amplitude increment at the

crossover point (or F_p -capture point) increases as F_p moves away from the fiber CF. This pattern, which we have called the *isocapture curve*, is plotted in Fig. 5 (the solid line). The threshold tuning curve of the fiber (dashed line) is also shown, shifted down by 13 dB (its threshold value, in SPL, at CF) so that the lowest point in the tuning curve coincides with the lowest increment intensity used (0 dB). One significant difference between these two curves is that, at frequencies lower than CF, the tuning curve is always above the isocapture curve. In a linear system, these two curves would be identical.²

As defined, the threshold tuning curve of a fiber indicates the effectiveness of each sinusoid in evoking the criterion response. Were the peripheral auditory system linear, its transfer function would be the inverse of the threshold curve (Greenberg *et al.*, 1986). The differences between the isocapture curve and the tuning curve show that, in the presence of a multitone background of 70 dB SPL, it requires less of an amplitude increment at a probe frequency below CF for that frequency to dominate the response pattern than is predicted from the inferred low-intensity transfer function. For instance, at an F_p of 1466 Hz, it required only a 15-dB increment for F_p to capture the response synchrony [Fig. 3(b)], yet the tuning curve indicates nearly a 30-dB difference in threshold sensitivity between CF and F_p . The system is obviously behaving in a nonlinear manner.

Figure 6 contains isocapture curves, together with the vertically shifted threshold tuning curves, for four other fibers for which we have such data. For two of the fibers [Fig.

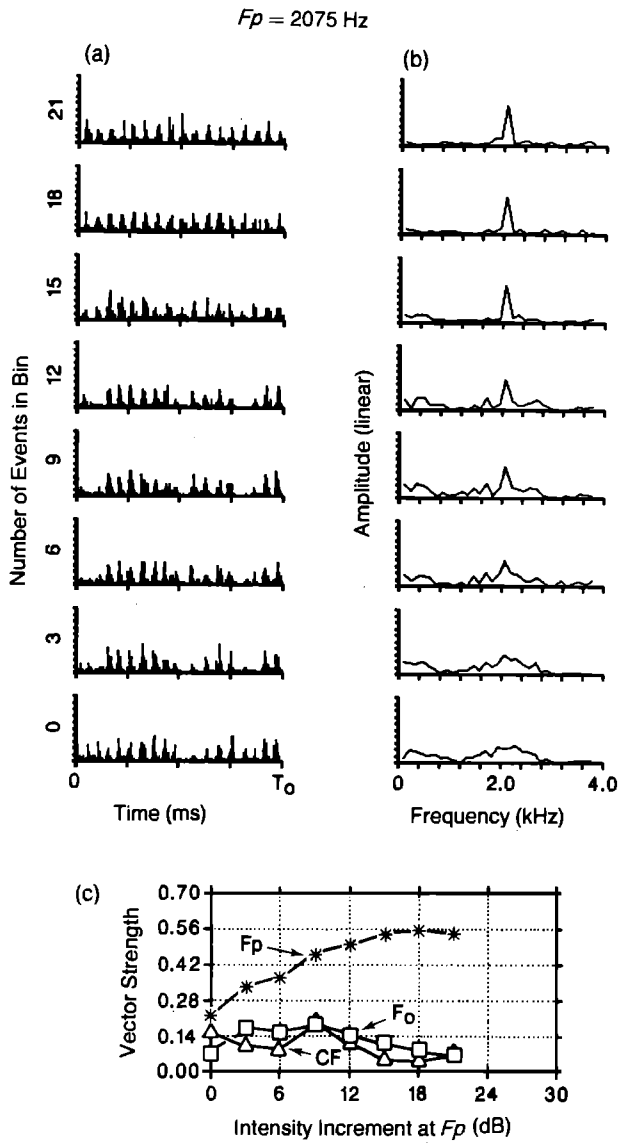


FIG. 4. (a) Period histograms of responses to random-phase multitone complexes with an F_p of 2075 Hz, for fiber A16. Amplitude increment at F_p given on the ordinate. (b) Magnitude spectra of the corresponding PHs in column (a). (c) Summary plots for vector strengths of F_0 , F_p , and CF, as functions of amplitude increment at F_p , for the data in column (b).

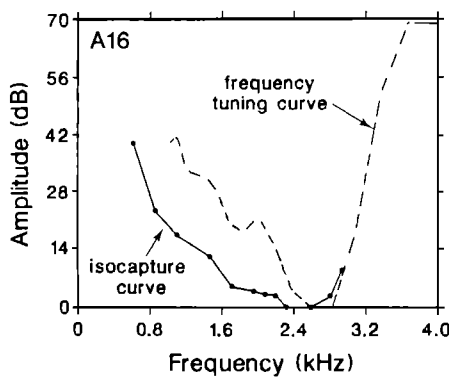


FIG. 5. Threshold frequency tuning curve (FTC) of fiber A16, shifted downwards by 13 dB (the threshold value in SPL) is shown as the dashed line. The solid line is the isocapture curve, formed by connecting the points (on a dB scale) at which the F_p and CF components share equal values of vector strength.

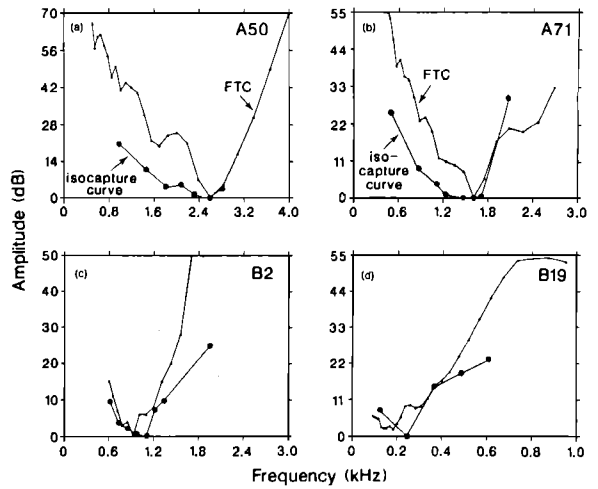


FIG. 6. Threshold frequency tuning curves (FTCs) shifted downwards to the 0-dB line (thin lines) and isocapture curves (thick lines) for four fibers: (a) fiber A50, CF = 2594 Hz, SR = 32/s, (b) fiber A71, CF = 1600 Hz, $15.6/s < SR < 20.4/s$, (c) fiber B2, CF = 925 Hz, SR = 15/s, (d) fiber B19, CF = 200 Hz, SR = 0.

6(a) and (b)], both with CFs above 1.5 kHz, the low-frequency limb of the isocapture curve lies significantly below that of the frequency threshold curve. For each of the other two fibers, both with CFs below 1 kHz [Fig. 6(c) and (d)], the shapes of the two curves seem to be similar, except at frequencies well above CF.

D. Effective bandwidth of peripheral filters

For a linear system, the isocapture curve defined above would be identical to the filter's frequency selectivity. If the fiber's threshold tuning curve is regarded as the fiber's frequency-selectivity function, then the above data strongly demonstrate that nonlinear effects are produced in the ear by the 70-dB SPL multitone background condition. One parsimonious interpretation of such a nonlinearity is that the bandwidth of the cochlear partition's filter is broadened by this sound background. Such an interpretation is consistent with intensity-dependent basilar-membrane tuning (Rhode, 1971; Robles *et al.*, 1985), with the formant-capturing phenomena reported in our first article (Deng and Geisler, 1987a), and with the modeling work described in the next article (Deng and Geisler, 1987b).

In a linear system, a flat-spectrum signal would result in a response whose amplitude spectrum profile would be proportional to the system's transfer function. One natural implication of our bandwidth-broadening interpretation of the probe-tone data is that the spectrum of the response to a flat-spectrum sound should also be broadened compared to that predicted from the threshold tuning curve. This is indeed the case. In Fig. 7(a), the response's spectral amplitudes at individual stimulus frequencies for flat-spectrum multitone stimuli of random phase and of zero phase are plotted (square and circle symbols, respectively). To compare the multitone response with the frequency selectivity measured by the threshold tuning curve and by the isocapture capability, the curves in Fig. 5(a) were turned upside down and shifted vertically by amounts required to superimpose their

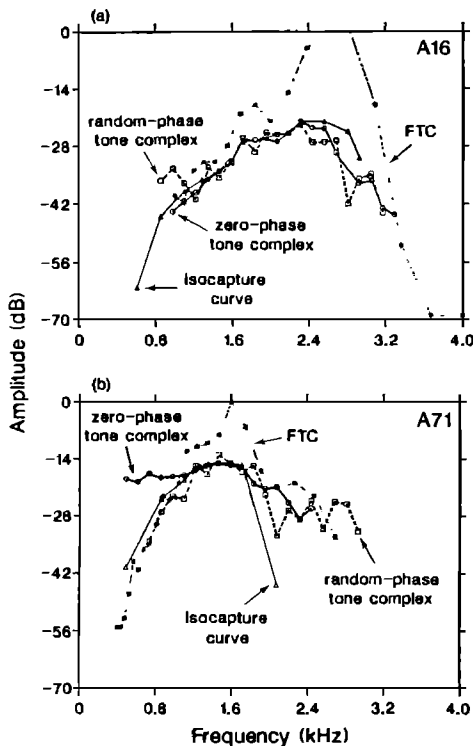


FIG. 7. (a) Four different frequency-selectivity measures are plotted for fiber A16. The threshold frequency tuning curve (FTC) and the isocapture curve, formed by inverting the curves of Fig. 5, are indicated by the asterisk and triangle symbols, respectively. The curves using circles and squares are the spectral magnitudes of the PHs in response to the zero-phase and random-phase complexes, shifted vertically to align their low-frequency limbs. (b) Four different frequency-selectivity measures are plotted for fiber A71. Asterisks, triangles, circles, and squares indicate the threshold frequency tuning curve (FTC), the isocapture curve, and the spectral magnitudes of the PHs in response to equiamplitude zero-phase and random-phase multi-tone complexes, respectively.

low-frequency sides. Although this type of display is different from those used by others (de Boer and de Jongh, 1978; Evans, 1985), we feel that it is useful, for it lines up those portions of the curves least likely to be affected by mechanical nonlinearities (cf. Rhode, 1978). Because the ordinate scales are in dB units, any such shifts preserve the shapes of the curves. As can be seen, the frequency selectivities exhibited by the fiber in response to the zero-phase and to the random-phase flat-spectrum signals are very similar to the selectivity manifested in the isocapture curve, particularly for frequencies below CF. However, all three suprathreshold curves are much broader than the threshold frequency selectivity obtained with sinusoidal signals. Further, the most sensitive frequency in each of the suprathreshold curves is somewhat below the threshold CF. All of these features are reminiscent of Rhode's figure showing basilar-membrane nonlinearities (1971, Fig. 6).

The frequency-selective characteristics of six other fibers were determined using the flat-spectrum multi-tone complexes. In most cases, the suprathreshold determinations produced curves broader than those of the threshold tuning curves (Deng, 1986). For one of these fibers, A71, the various frequency-selectivity curves are plotted in Fig. 7(b). Except for one point above CF, the shape of the fre-

quency-selectivity curve obtained using the random-phase flat-spectrum multi-tone complexes (squares) is very similar to that of the isocapture curve (triangles). However, for this fiber, the frequency-selectivity curve derived from the zero-phase flat-spectrum multi-tone complex is much broader on the low-frequency side of CF (circles) than all of the others. This striking difference between zero-phase and random-phase responses, the only such example in our small data set, may be due to the different types of waveforms associated with the two flat-amplitude stimuli. The random-phase stimulus resembles random noise [cf. Fig. 1(b)] and discharge probabilities are distributed fairly uniformly throughout the entire fundamental period [cf. Fig. 4(a), bottom panel]. The zero-phase stimuli, by contrast, appear to be bipolar pulses [cf. Fig. 1(a)] and produce response probabilities that are clustered within the fundamental period in a waveform similar to click responses [cf. Fig. 2(f), bottom panel]. The known distorting effects that neural refractoriness has upon click responses (cf. Gray, 1967) may account, at least in part, for the broad spectrum of the zero-phase responses of this fiber.

E. Frequency suppression nonlinearities

As has been demonstrated in the previous sections, the apparent broadening of a fiber's frequency selectivity at high input intensities may underlie the mechanisms by which a spectral peak in a stimulus can capture a fiber's response synchrony to a larger degree than that implied by its threshold tuning curve. This "enhancement" of the response to a spectral peak occurs not only because the response synchrony to it grows with increasing spectral height, but because the spectral peak actually suppresses the strengths of the fiber's synchronization to other frequency components.

Figure 8 presents four representative examples. The first [Fig. 8(a)] concerns fiber B2, with a CF around 950 Hz. Random-phase multi-tone complexes with the amplitude of the 7th harmonic (854.5 Hz) incremented by 0 (flat), 5, 10, 15, and 20 dB were presented. The FFT spectra of the response PHs were calculated for all five conditions. Note that, as the amplitude of the 854.5 Hz (F_p) component rises, the amplitude of the response component at this frequency does not grow, except for the lowest (5-dB) increment condition. Rather, the spectral amplitudes of the other harmonics decrease dramatically. This reduction in synchronization is particularly evident for the F_0 component and for harmonics close to F_p . For larger probe-tone increments, the suppression is even greater, reaching -28 dB at 977 Hz when a 20-dB F_p increment is used. Similar features are seen in the other response profiles shown in Fig. 8, for fibers B2 (b) and A16 (c) and (d). It seems likely that the suppression in these figures is due, at least in part, to the automatic-gain-control (AGC) characteristics of the auditory periphery (Geisler and Greenberg, 1986). As the F_p component grows large in comparison to other components passed by the filter operative at that cochlear point, it tends to set the gain of the AGC.

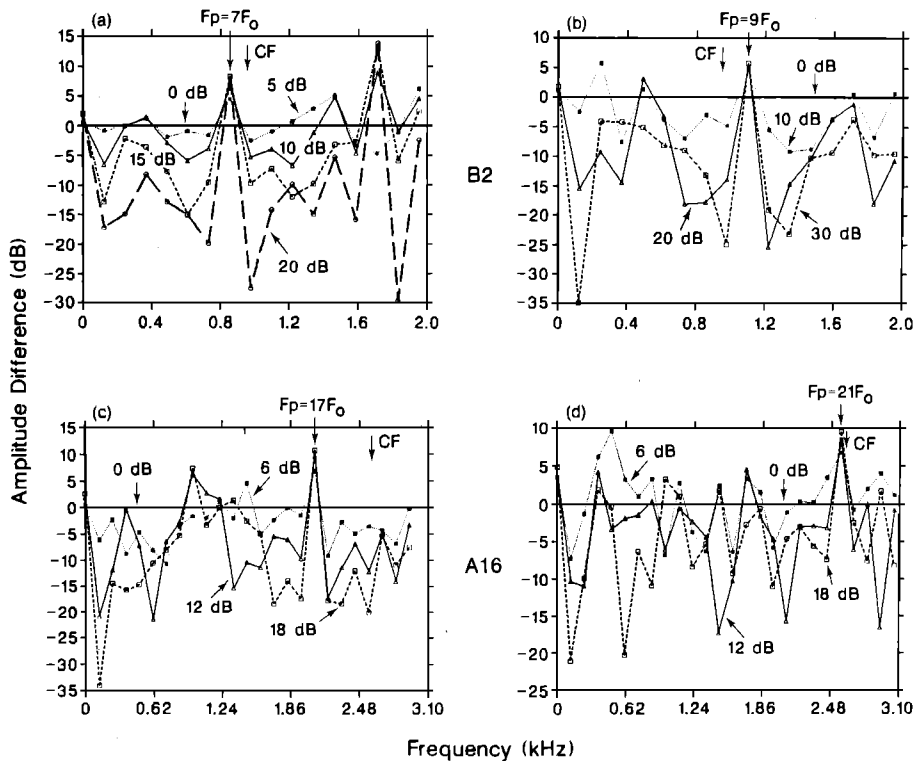


FIG. 8. Normalized amplitude spectra obtained from the PHs produced by multitone complexes in fiber B2 [(a) and (b)] and A16 [(c) and (d)], showing that, despite the limited dynamic range of synchrony, a relatively large range of F_p amplitudes can be encoded by the orderly reduction of the fiber synchronies to frequencies other than F_p itself. For each panel, the spectral amplitudes of the response PHs were calculated, and, for each frequency, the ratios of their resulting amplitudes compared to those resulting from the 0-dB increment (i.e., equiamplitude) case are plotted, on a dB scale: (a) random-phase case, $F_p = 854.4$ Hz, F_p increments were 5, 10, 15, and 20 dB, fiber B2; (b) random-phase case, $F_p = 1099$ Hz, F_p increments were 10, 20, and 30 dB, fiber B2; (c) zero-phase case, $F_p = 2075$ Hz, F_p increments were 6, 12, and 18 dB, fiber A16; (d) zero-phase case, $F_p = 2563$ Hz, F_p increments were 6, 12, and 18 dB, fiber A16.

F. Comparisons with the neural responses to speech stimuli

One impetus of the present study comes from our work on the responses of these fibers to speech syllables (Deng and Geisler, 1987a), where one particular formant was often found to dominate the temporal responses of fibers having a wide range of CF. Important issues raised by such observations concern the specification of conditions under which such broad dominance occurs, and whether a large relative spectral amplitude of the formant is the primary factor that causes a dominant response. More fundamentally, our goal is to relate the formant-dominant responses to the basic frequency selective and suppressive properties of the fibers.

These issues are approached in light of the insights gained from the features of fiber responses to multitone complexes demonstrated in the previous sections. In particular, the isocapture curve, as a measure of a fiber's frequency selectivity, divides the stimulus space formed by frequency and amplitude increment into a *capture area* and a *subcapture area*, corresponding to the spaces above and below the curve, respectively (cf. Fig. 5). If an incremented probe component in an otherwise spectrally flat multitone signal serves as a valid abstract of a speech formant, the isocapture property derived from the multitone responses should provide a means of accounting for a fiber's formant-dominant responses to speech.

In this section, we show, using two examples, that, under comparable stimulus intensities, the multitone stimuli with amplitude-incremented probe tones produce responses with synchrony patterns comparable to those evoked by the corresponding speech signals. In this paradigm, the F_p component was chosen to be near a formant frequency, and the amount of the increment in the F_p amplitude was set com-

parable to the formant height in the speech sound.

In the following example, the "formant height" is defined, for fiber A16, as the amplitude difference (in dB) between the second and third formants of the vocalic portion of the syllable /nu/ produced by speaker ST. This definition is a consequence of the fiber's CF, 2600 Hz being close to F_3 [Fig. 9(a)]. The CF tone will be the most effective one of the local multitones in determining response synchrony, as will F_3 be in the speech-stimulus case. In the example with fiber A71, the fiber's CF of approximately 1600 Hz falls between F_2 and F_3 during the later vocalic portion of /nu/; under such conditions, the definition of formant height given above clearly underestimates the difference in amplitude between F_2 and the frequency components near the fiber's CF.

Figure 9(a) is the stimulus spectrogram of /nu/ (ST), which was presented at an intensity of 72 dB SPL. Fiber A16's response spectrogram is shown in (d), and A71's in (g). Figure 9(b) is the amplitude spectrum of the sound during the 80- to 110-ms segment, where F_2 , at approximately 1700 Hz, is 10 dB higher in amplitude than F_3 , near 2500 Hz. The multitone signal related to this speech segment is one with a 10-dB increment in the amplitude of the tone having a frequency of 1709 Hz ($F_p = 14$ th harmonic of F_0). According to the isocapture curve of this fiber (Fig. 5), the combination of an F_p of 1709 Hz and an amplitude increment of 10 dB is clearly within the capture area. Thus F_p would dominate the response synchrony of the fiber for that stimulus. This domination is illustrated by the response profiles shown in Fig. 9(e), for F_p increments of 12 and 9 dB, respectively. In both cases, which together bracket the 10-dB-increment condition, the dominant frequency component in the response is F_p . Assuming that this multitone signal with a probe component that is 10 dB above the others is

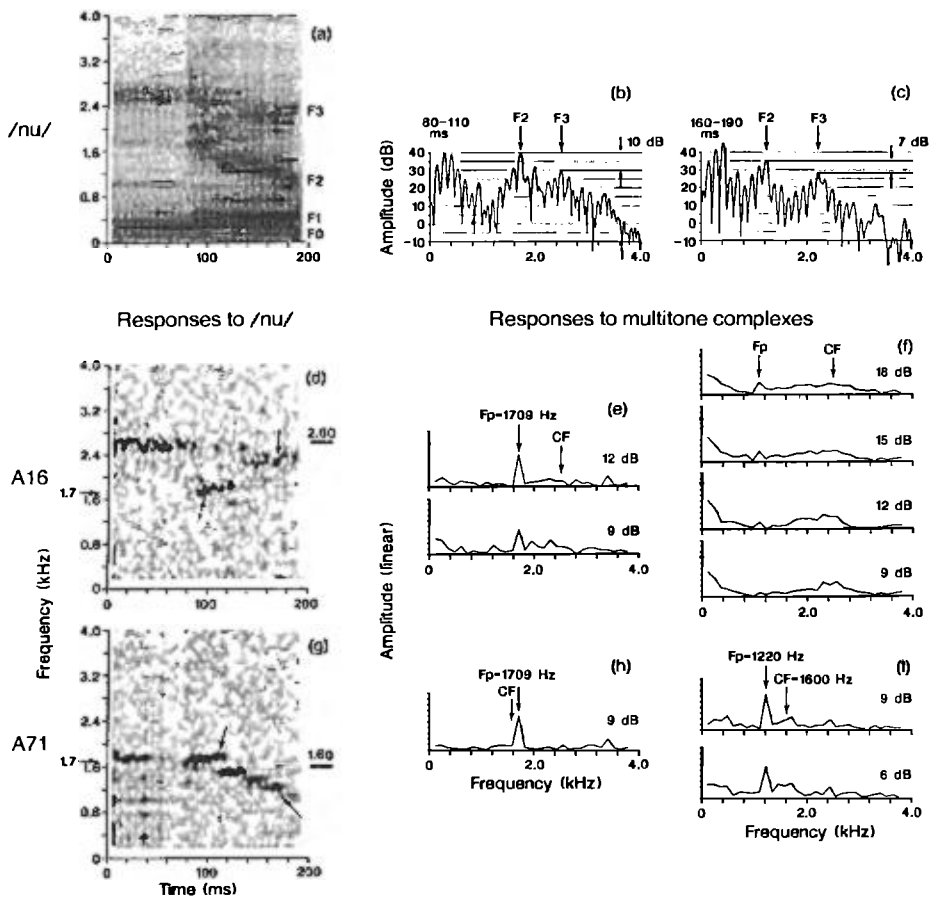


FIG. 9. Responses of two fibers to syllable /nu/ (ST) and related multitone complexes. Top row: stimulus /nu/ (ST). (a) Spectrogram. (b) Spectral amplitudes over the 80- to 110-ms segment (a beginning vocalic portion). Frequencies F_2 and F_3 , and the 10-dB formant height, are indicated. (c) Spectral amplitudes over the 160- to 190-ms segment. It is seen that F_2 has moved significantly downwards, and the formant height has been reduced to 7 dB. Middle row: responses of fiber A16. (d) Spectrogram of response PSTH to /nu/ (ST). Dominant synchronization by F_2 (near 100 ms) and by F_3 (near 170 ms) indicated by arrows. CF = 2600 Hz. (e) Spectral amplitudes of response PHs to zero-phase multitone complexes having F_p at 1709 Hz (comparable to the F_2 in speech) and F_p -amplitude increments of 9 and 12 dB (comparable to the 10-dB formant height in the speech signal), respectively. The F_2 is considerably below the CF of A16 (near 2600 Hz). (f) Spectral amplitudes of response PHs to zero-phase multitone complexes having F_p at 1099 Hz [as close as possible to the F_2 in /nu/ (ST) just after the end of the murmur] and F_p -amplitude increments of 9, 12, 15, and 18 dB, respectively. Even though such increments are higher than the 7-dB formant height, it is the frequency component near the fiber's CF, instead of F_p , that dominates the fiber's response. Bottom row: responses of fiber A71. (g) Spectrogram of response PSTH to /nu/ (ST). Dominant synchronization by F_2 indicated by arrow (near 110 ms and near 180 ms). CF = 1600 Hz. (h) Spectral amplitudes of response PH to a zero-phase multitone complex having F_p at 1709 Hz and an F_p -amplitude increment of 9 dB. (i) Spectral amplitudes of response PHs to zero-phase multitone complexes, having F_p at 1220 Hz and F_p -amplitude increments of 6 and 9 dB, respectively.

an appropriate analog of the 80- to 110-ms segment of the sound /nu/, we would predict that the 10-dB formant height is enough to produce synchrony capture by F_2 . As predicted, the responses of the fiber during that time segment were strongly synchronized to energy in a small band located near 1700 Hz [Fig. 9(d)]. Moreover, the isocapture curve would predict further potentialities of F_2 dominance in this case, as the 10-dB formant height is still 4 dB above this frequency's capture/subcapture boundary of 6 dB.

Similar response synchrony patterns are also seen in the spectrogram of fiber A71's responses during the 80- to 110-ms segment [Fig. 9(g)], and in the amplitude spectra of the response PHs to the multitones with a 9-dB increment in the amplitude of the F_p component [Fig. 9(h)]. The fiber strongly synchronizes to frequency components near 1.7 kHz in its responses to both the speech sound and its multitone analog. In this case, 9 dB is approximately the differ-

ence between the amplitude of F_2 and the largest neighboring harmonic peak, and so is an appropriate increment for F_p 's amplitude. Other multitone response data (Deng 1986, Fig. II-5f) infer that the synchrony to F_2 during this segment would be so robust that even a 3-dB formant height would produce F_2 dominance.

During the 160- to 190-ms interval for /nu/, F_2 recedes from F_3 , and the formant height drops to 7 dB [Fig. 9(c)]. One consequence of this F_2 transition is that the multitone signal related to this new segment of speech would be placed outside the capture area of fiber A16, about 8 dB below the capture/subcapture boundary. Examples of response spectral profiles used in establishing this boundary point at 1099 Hz (the F_p closest to F_2 in our data) are shown in Fig. 9(f). Clearly, a 9-dB increment is far below that needed for F_p to obtain dominant synchrony in the response profile. Thus we would predict that F_2 during the 160-190 segment of /nu/

would be too weak to capture the fiber's discharge synchrony. Indeed, Fig. 9(d) shows that, instead of maintaining synchrony to $F2$, fiber A16 weakly synchronizes to $F3$ during this segment. Extrapolations from the multitone responses [Fig. 9(f)] suggest that the failure of $F2$ to capture fiber synchrony in this case is principally due to the larger difference between the frequencies of $F2$ and CF, with the reduction in formant height playing a secondary role.

Fiber A71's discharges, by contrast, do synchronize to $F2$ during the 160- to 190-ms interval [Fig. 9(g)]. An examination of that fiber's responses to multitone signals having an Fp of 1220 Hz, shown in Fig. 9(i), indicates that Fp dominates the response synchrony even with only a 6-dB increment. The capture/subcapture boundary obviously lies below that. Thus it is expected that $F2$, with a formant height (relative to fiber CF) of much greater than 7 dB, would dominate the response synchrony in that segment of the response, as indeed it does.

From this and several other examples in our larger data set (Deng, 1986), we suggest the following conclusions. The dominance of a fiber's discharges by a low-frequency speech formant is usually mimicked in the fiber's response to an analogous multitone complex, regardless of the details of other frequency components. This analogous signal should have a similar overall sound intensity, an Fp similar to the formant frequency, and an increment in the Fp amplitude that is similar to the formant height. In other words, we conclude that the widespread formant-dominant feature of auditory-nerve fibers' responses to certain speech sounds results from the formant acting as a large, isolated energy peak.

III. DISCUSSION

A. Summary and implications of the results

This study represents an effort to bridge such nonlinear effects as "strong-component capture," observed in auditory-nerve fiber responses to speech signals (Young and Sachs, 1979; Sinex and Geisler, 1983; Delgutte and Kiang, 1984; Carney and Geisler, 1986; Deng and Geisler, 1987a), and the basic frequency selective and suppressive properties of the fibers, which have been explored extensively in the literature using relatively simpler single-tone and two-tone stimuli (e.g., Johnson, 1980; Javel *et al.*, 1983; Greenberg *et al.*, 1986). The multitone complexes used in the present study provide a particularly useful tool for quantitatively investigating the basic characteristics of auditory-nerve-fiber response synchronization.

The most basic results reported in this article concern the relationships of a fiber's discharge synchronization to various frequency components and to the values of the amplitude increments at the probe frequency. Among these relationships, the one between the increase of the fiber's synchrony to Fp and the decrease of the synchrony to CF, with increasing amounts of the probe-amplitude increment, has received the most detailed investigation. At some point, an equality of these two synchronizations, one growing and one diminishing, is reached. A collection of such points forms an isocapture curve (e.g., Fig. 5), from which the ability of the Fp component to dominate the neural discharge synchroni-

zation can be readily obtained. Due to this property, we have interpreted the isocapture curve to be a measure of the "strong-component capture" ability of the fiber. At each Fp point on the abscissa, the lower the ordinate value of a point on the curve is, the stronger the capture ability of that tone will be.

On the other hand, the isocapture curve describes the frequency-selective property of the fiber, provided that we are willing to accept the synchronization magnitude as a measure of the neural response. Such a measure has indeed been used extensively in the past in investigations of auditory-nerve fiber responses to single tones, where it has been shown that the shape of the threshold frequency tuning curve based on single-tone synchrony resembles that based on the traditionally used discharge rate (Johnson, 1980; Javel *et al.*, 1983). Due to synchrony saturation at high sound levels, the synchrony obtained with many successively applied single-tone stimuli would fail to provide much frequency-selectivity information about the fiber. Yet with multi-component stimuli, a fiber's frequency-selective property is demonstrable even at the highest intensities, for different frequency components in the stimulus are represented differentially in the spectral profile of the response. The advantage of this approach is that it provides a means of reliably estimating the frequency tuning capabilities of a fiber at high sound levels, without it being obscured by such effects as the saturations of discharge rate and vector strength. This interpretation of the isocapture curve as a measure of a fiber's frequency selectivity is reinforced by our finding that isocapture curves are very similar in shape to the spectral response profiles resulting from multitone stimuli having flat spectral envelopes (cf. Fig. 7).

For us to entertain both of these points of view simultaneously, we have come to regard the different regions of the probe tone's frequency/amplitude-increment plane as dominated by different nonlinear mechanisms. In the subcapture region, where no member of the stimulus ensemble dominates, we believe that the nonlinearities principally operative are those connected with the hydromechanical vibrations of the cochlea. No actual suppression of particular components is envisioned; rather, the sharpness of the cochlear resonance is reduced and the bandwidth accordingly increased, as Rhode (1978) has observed for basilar-membrane vibrations. In the captive region, by contrast, where one component dominates the response spectrum, the principal nonlinearity appears to be of the automatic-gain-control variety in which the hair-cell/nerve-fiber complex has been implicated (Geisler and Greenberg, 1986). In such cases, the dominant peak within the fiber's bandwidth appears to set the gain of the system and so cause the actual suppression of other frequency components (cf. Fig. 8). According to this analysis, the suppressive effects would just be coming into play at the isocapture point. While suppressive effects can be exerted by tones at intensities lower than those that cause excitation (Sachs and Kiang, 1968), on the low-frequency side of CF these tend to occur when the added tone is considerably more intense (as much as 40 dB more than the excitatory tone). Thus, for fibers with high spontaneous rates (high-SR fibers), for which we detected no cases of rate suppression as

the amplitude of F_p was raised, the scheme presented above appears to account for the response synchrony patterns produced by speech and speechlike stimuli. For low/medium-SR fibers, in which suppressive effects are much stronger, this scheme is obviously not adequate.

B. Comparisons with previous studies

Multitone complexes with a flat spectral envelope have been used in several previous studies. Smoorenburg and Linschoten (1977) recorded from cochlear nucleus neurons using a complex of 63 equiamplitude harmonics, all in cosine phase. In their example, the neural bandwidth derived by using this complex at sound intensities comparable to ours is considerably broader than that which can be derived from the neuron's single-tone response area.

Evans (1981, 1985) apparently was the first to apply equiamplitude tone complexes to studies of auditory-nerve fibers. Like us, he used both constant-phase and random-phase conditions. One of his principal conclusions was that, at least for fibers with CFs below 1.5 kHz, the multitone frequency-selectivity curves of fibers in the cat auditory nerve were very similar in shape to their respective threshold tuning curves over a wide intensity range. Results obtained using random-noise stimuli (de Boer and De Jongh, 1978; Evans, 1985) support that conclusion. In fact, some of the results from our own laboratory obtained with pairs of tones having equal amplitudes (Greenberg *et al.*, 1986) also demonstrate similar intensity-independent characteristics. Our data from low-CF fibers [Fig. 6(c) and (d)] are consistent with the previous results. However, data drawn from fibers with CFs greater than about 1.2 kHz [Fig. 6(a) and (b)] show considerable differences between threshold and suprathreshold frequency selectivities. For such higher CF fibers, Evans (1985) also reports that, at least for intensities that exceed threshold by more than 40–60 dB, effects similar to the ones we described occur: The effective filter shape broadens on the low-frequency side and there is a downward shift of the center frequency. Although possible species differences make direct comparisons risky, such changes have also been reported in the suprathreshold frequency selectivities of rat auditory-nerve fibers subjected to wideband noise stimuli (Møller, 1977).

An additional confounding factor in high-frequency data concerns the drop-off in the synchronization ability of auditory-nerve fibers that occurs at these frequencies (Johnson, 1980). A 3-kHz fiber, for example, develops a maximum synchronization coefficient to its CF tone of about 0.5, as opposed to values in excess of 0.8 demonstrated by lower frequency fibers. Thus equal synchronization values for two frequency components in the neural response waveform need not imply that the two frequencies are equally represented in the ciliary deflections of the inner hair cell. However, because of the small differences that occur between CF and the frequencies of the higher frequency points in our relevant isocapture curves [Figs. 5 and 6(a) and (b)], this synchronization drop-off is thought to have a negligible effect upon the present study.

Two other studies using flat-spectrum multitone stimuli reported that the response spectra obtained at low intensities

of presentation resembled threshold tuning curves (Horst *et al.*, 1985, 1986). From their figures, the response spectra indeed broadened at high intensities (e.g., see Fig. 3 in Horst *et al.*, 1985). Due to the spectral "edges" present in their multitone stimuli (they only included components within a 1-oct band in their stimuli, as edge effects were the focus of their studies), it is not certain whether these edge effects, or intensity-dependent nonlinear effects on the filter bandwidth itself, were responsible for such observed broadening.

The only study prior to ours that used multitones with one component's amplitude incremented has appeared only recently (Horst *et al.*, 1985). This study was very brief, citing results from only one fiber, with only one probe component (at the fiber's CF), and with only three levels of the amplitude increment. The incompleteness of their probe-tone data does not allow a detailed comparison to be made with our data. However, their data showing that the component whose amplitude was incremented by even a small amount tended to dominate the response by suppressing other components, such as those due to "edge effects," is consistent with some of our results.

C. Relevance to "profile analysis"

The present study has shown that small increments in the sound-pressure level of low-frequency components are detectable in the spatio-temporal excitation patterns of auditory-nerve fibers. In particular, increments as small as 2 dB are effective in "capturing" the timing behavior of single fibers in tonotopic proximity to the probe component [cf. Fig. 3(e)]. Substantially larger probe increments are required to modify the synchrony patterns of fibers with distant CFs.

This finding is of potential relevance to the "profile analysis" studies of Green and associates (Green, 1983; Green *et al.*, 1984; Green and Forest, 1986; Green and Mason, 1985; Mason *et al.*, 1984) in which human listeners were required to detect small increments of a probe component amidst a background signal of equal-amplitude tones. In these psychoacoustic studies, listeners could detect increments between 1 and 2 dB in size, particularly for probe frequencies below 3 kHz. The near identity of the psychoacoustic and the physiological probe-increment thresholds is striking. Among several suggested alternatives, it supports the possibility that the human judgments are made by central nervous system monitoring of the discharge synchrony of just a small group of fibers having CFs near the probe-tone frequency.

One feature of the psychoacoustic data that is consistent with synchrony coding is the relative invariance of probe-increment threshold to random variations in the sound-pressure level of the background signal. In previous publications, it was shown that the synchrony-based frequency selectivity of some auditory-nerve fibers is also relatively invariant over wide dynamic ranges (e.g., Greenberg *et al.*, 1986), consistent with a mechanism functionally equivalent to an AGC (Geisler and Greenberg, 1986). Thus the synchrony information available from a small localized group of fibers would also be relatively intensity invariant. The fact that the probe-increment detection threshold increases above 3 kHz is also consistent with a synchrony hypothesis, for peripheral

synchronization ability diminishes above this frequency, at least in the cat (Johnson, 1980).

One major characteristic of the psychoacoustic observations that is difficult to account for with the hypothesis that the essential information regarding probe-tone increments is carried by a tonotopically localized group of fibers is the decrease in probe-increment detection threshold that occurs as the bandwidth of the background signal is increased. Although some auditory-nerve fibers have suprathreshold synchrony-derived response areas extending more than an octave on either side of CF (cf. Fig. 7), they are not responsive over the entire 3- to 4-oct range in which the component comparisons appear to occur. Nevertheless, the rather sharp sensitivity of the psychoacoustic judgments to the frequency spacing of the background components implies that synchrony information does indeed play an important role. Further experiments will be needed to identify just exactly which discharge characteristic(s) of the auditory-nerve fibers can fully account for the probe-increment detection abilities of human observers.

ACKNOWLEDGMENTS

This work, based, in part, on L. Deng's doctoral thesis (1986), was supported by NIH Program Project Grant NS-12732. We would like to thank Ravi Kochhar for essential aid in the stimulus-generation programs. Tom Yin's useful insight into implications of the isocapture curve is appreciated. We would also like to thank Laurel Carney, Joseph Hind, Duck Kim, and William Rhode for reading and criticizing earlier versions of this article. We appreciate the help of Carol Dizack, Holly Jackson, and Terry Stewart in preparing the manuscript.

¹Because the temporal resolution of the digitally synthesized multitone complex was taken as $50 \mu\text{s}$ [the same as the sampling interval in our speech stimuli (Deng and Geisler, 1987a)], and a 4096-point FFT was used in the analysis, the total duration of the sample was 0.2048 s. This corresponds to a basic frequency resolution of 4.8828 Hz. The 25th harmonic of that resolution is 122.07 Hz. Using the latter frequency as the fundamental component F_0 of the stimulus ensemble insured that the sample window is exactly $n \times 25$ ($n = 1, 2, \dots, 60$) times the period of the n th component in the stimulus. Thus errors due to the spread of spectral lines by the windowing were eliminated. With 60 harmonics of this 122.07-Hz fundamental present, the signal's frequency spectrum extended up to 7324.2 Hz (122.07×60).

²To show this identity, assume that it takes 10 dB SPL of tone A to produce a synchronized response rate (the amplitude of the frequency-A component of the FFT of the PH) of 10 spikes/s, and that it takes 20 dB SPL of tone B to achieve this same "threshold" value of synchronized response rate. If tone A were now presented at 50 dB SPL, the synchronized rate in a linear system would grow to 1000 spikes/s. Tone B would have to be presented at 60 dB SPL to obtain that same synchronized rate. Thus the difference in threshold intensities (10 dB) is equal to the difference in suprathreshold intensities needed to obtain equal output amplitudes (Q.E.D.). To be sure, our threshold curves were determined by response-rate crite-

ria, not from synchronized-response rates, but data from Johnson (1980) and Javel *et al.* (1983) indicate that, for any one fiber, these two response curves have very similar shapes.

- Arthur, R. M. (1976). "Harmonic analysis of two-tone discharge patterns in cochlear nerve fibers," *Biol. Cybern.* **22**, 21-31.
- Carney, L. H., and Geisler, C. D. (1986). "A temporal analysis of auditory-nerve fiber responses to spoken stop consonant-vowel syllables," *J. Acoust. Soc. Am.* **79**, 1896-1914.
- de Boer, E., and de Jongh, H. R. (1978). "On cochlear encoding: Potentialities and limitations of the reverse-correlation technique," *J. Acoust. Soc. Am.* **63**, 115-135.
- Delgutte, B., and Kiang, N.Y.-S. (1984). "Speech coding in the auditory nerve: I. Vowel-like sounds," *J. Acoust. Soc. Am.* **75**, 866-878.
- Deng, L. (1984). "Phase response of cat auditory-nerve fibers to low-frequency tones: Effects of two-tone suppression, sound exposure and adaptation," M.S. thesis, University of Wisconsin—Madison, Madison, WI.
- Deng, L. (1986). "Experimental and modeling studies of complex sound processing in the peripheral auditory system," Ph.D. thesis, University of Wisconsin—Madison, Madison, WI.
- Deng, L., and Geisler, C. D. (1987a). "Responses of auditory-nerve fibers to nasal consonant-vowel syllables," *J. Acoust. Soc. Am.* **82**, 1977-1988.
- Deng, L., and Geisler, C. D. (1987b). "A composite auditory model for processing speech sounds," *J. Acoust. Soc. Am.* **82**, 2001-2012.
- Evans, E. F. (1981). "The dynamic range problem: Place and time coding at the level of cochlear nerve and nucleus," in *Neuronal Mechanisms of Hearing*, edited by J. Syka and L. Aitkin (Plenum, New York), pp. 69-85.
- Evans, E. F. (1985). "Aspects of the neural coding of time in the mammalian peripheral auditory system relevant to temporal resolution," in *Time Resolution in Auditory Systems*, edited by A. Michelsen (Springer, Berlin), pp. 74-95.
- Geisler, C. D., and Greenberg, S. G. (1986). "A two-stage nonlinear cochlear model possesses automatic gain control," *J. Acoust. Soc. Am.* **80**, 1359-1363.
- Goblick, T. J., and Pfeiffer, R. R. (1969). "Time-domain measurements of cochlear nonlinearities using combination click stimuli," *J. Acoust. Soc. Am.* **46**, 924-938.
- Goldberg, J. M., and Brown, P. B. (1969). "Response of binaural neurons of dog superior olivary complex to dichotic tonal stimuli: Some physiological mechanisms of sound localization," *J. Neurophysiol.* **32**, 613-636.
- Gray, P. R. (1967). "Conditional probability analysis of the spike activity of single neurons," *Biophys. J.* **7**, 759-777.
- Green, D. M. (1983). "Profile analysis: A different view of auditory intensity discrimination," *Am. Psychol.* **38**, 133-142.
- Green, D. M., Mason, C. R., and Kidd, G., Jr. (1984). "Profile analysis: Critical bands and duration," *J. Acoust. Soc. Am.* **75**, 1163-1167.
- Green, D. M., and Mason, C. R. (1985). "Auditory profile analysis: Frequency, phase, and Weber's law," *J. Acoust. Soc. Am.* **77**, 1155-1161.
- Green, D. M., and Forest, T. (1986). "Profile analysis and background noise," *J. Acoust. Soc. Am.* **80**, 416-421.
- Greenberg, S. G., Geisler, C. D., and Deng, L. (1986). "Frequency selectivity of single cochlear-nerve fibers based on the temporal response pattern to two-tone signals," *J. Acoust. Soc. Am.* **79**, 1010-1019.
- Greenwood, D. D. (1986). "What is synchrony suppression?," *J. Acoust. Soc. Am.* **79**, 1857-1872.
- Horst, J. W., Javel, E., and Farley, G. R. (1985). "Extraction and enhancement of spectral structure by the cochlea," *J. Acoust. Soc. Am.* **78**, 1898-1901.
- Horst, J. W., Javel, E., and Farley, G. R. (1986). "New effects of cochlear nonlinearity in temporal patterns of auditory nerve fiber responses to harmonic complexes," in *Peripheral Auditory Mechanics*, edited by J. B. Allen, J. L. Hall, A. Hubbard, S. T. Neely, and A. Tubis (Springer, Berlin), pp. 298-305.
- Houtgast, T. (1974). "Lateral suppression in hearing," Doctoral thesis, Free University of Amsterdam, The Netherlands.
- Javel, E., McGee, J., Farley, G. R., and Gorga, M. P. (1983). "Suppression of auditory nerve responses. II. Suppression threshold and growth, iso-suppression contour," *J. Acoust. Soc. Am.* **74**, 801-813.
- Johnson, D. H. (1980). "The relationship between spike rate and synchrony in responses of auditory-nerve fibers to single tones," *J. Acoust. Soc. Am.* **68**, 1115-1122.
- Lieberman, M. C. (1978). "Auditory-nerve response from cats raised in a low-noise chamber," *J. Acoust. Soc. Am.* **63**, 442-455.

- Mason, C. R., Kidd, G. Jr., Hanna, T. E., and Green, D. M. (1984). "Profile analysis and level variation," *Hear. Res.* **13**, 269-275.
- Møller, A. R. (1977). "Frequency selectivity of single auditory-nerve fibers in response to broadband noise stimuli," *J. Acoust. Soc. Am.* **62**, 135-142.
- Pickett, J. M. (1980). *The Sounds of Speech Communication; A Primer of Acoustic Phonetics and Speech Perception* (University Park, Baltimore, MD).
- Rhode, W. S. (1976). "A digital system for auditory neurophysiological research," in *Current Computer Technology in Neurobiology*, edited by P. Brown (Halstead, New York), pp. 543-567.
- Robles, L., Ruggero, M. A., and Rich, N. C. (1986). "Basilar membrane mechanics at the base of the chinchilla cochlea. I. Input-output functions, tuning curves, and response phases," *J. Acoust. Soc. Am.* **80**, 1364-1374.
- Rose, J. E., Brugge, J. F., Anderson, D. J., and Hind, J. E. (1967). "Phase-locking response to low frequency tones in single auditory nerve fibers of the squirrel monkey," *J. Neurophysiol.* **30**, 769-793.
- Sachs, M. B., and Kiang, N. Y.-S. (1968). "Two-tone inhibition in auditory-nerve fibers," *J. Acoust. Soc. Am.* **43**, 1120-1128.
- Schroeder, M. R., Atal, B. S., and Hall, J. L. (1978). "Optimizing digital speech codes by exploiting masking properties of the human ear," *J. Acoust. Soc. Am.* **66**, 1647-1652.
- Sinex, D. G., and Geisler, C. D. (1983). "Responses of auditory-nerve fibers to consonant-vowel syllables," *J. Acoust. Soc. Am.* **73**, 602-615.
- Smooenburg, G. F., and Linschoten, D. H. (1977). "A neurophysiological study on auditory frequency analysis of complex tones," in *Psychophysics and Physiology of Hearing*, edited by E. F. Evans and J. P. Wilson (Academic, New York), pp. 175-183.
- Young, E. D., and Sachs, M. B. (1979). "Representation of steady-state vowels in the temporal aspects of the discharge patterns of populations of auditory-nerve fibers," *J. Acoust. Soc. Am.* **66**, 1381-1403.